Olivine as a reactive aggregate in lime mortars

Paul Westgate, Kevin Paine, Richard J Ball

BRE Centre for Innovative Construction Materials, Department of Architecture and Civil Engineering, University of Bath, Bath, BA2 7AY, UK

Keywords: olivine, forsterite, aggregate, mortar, carbon dioxide, carbonate, CO_2 emissions

Abstract

This paper presents the first investigation into the use of olivine as an aggregate material for calcium lime mortars. Lime binders provide many advantages when compared to cement binders such as higher vapour permeability and the ability to accommodate movement. They are undergoing a resurgence in their use in the conservation of historic buildings and in combination with environmentally friendly natural materials where these attributes are particularly important. Their ability to mitigate against global warming through the sequestration of CO_2 by carbonation is a further advantage which will bring positive environmental impact.

The equilibrium reaction products between non-hydraulic lime and olivine were calculated using the thermodynamic software GEMS3 Selektor. Experimental mortar mixes were modelled with varying ratios of quartz sand aggregate and olivine sand aggregate. The software predicted phase assemblage at equilibrium comprising calcite, dolomite, magnesite and quartz, with mass percentages depending on the ratio of quartz to olivine.

The mortars morphological, chemical and mechanical properties were evaluated using Scanning electron microscopy, X-ray diffraction (XRD), Raman spectroscopy, thermogravimetric analysis (TGA) and compressive strength testing. Significantly, this study has shown that the use of olivine based aggregates in finely divided form can enhance carbonation, and hence the CO_2 absorption capacity of these mortars. Dolomite formed within the mortar from the reaction of olivine aggregate with lime and carbon dioxide in the presence of moisture. The superior mechanical properties and increase in compresive strength from 0.5 to 2.5 MPa was attributed to the dolomite formed through carbonation.

1. Introduction

The continued high level of greenhouse gas emissions and its effect on the environment continues to be a major cause for concern. The International Panel on Climate Change (IPCC) has warned that continued emission of greenhouse gases will cause long-lasting changes to the climate system, increasing the likelihood of severe, pervasive and irreversible impacts for people and ecosystems [1]. One of the strategies being investigated to mitigate the effects of greenhouse gas emissions is the capture and storage of carbon dioxide, whereby carbon dioxide is captured from the atmosphere and stored in underground sites such as former gas and oil fields and in porous rock formations [2]. More recently, there has been much interest in capturing carbon dioxide by utilizing calcium and magnesium containing minerals to form carbonates [3]. This method of sequestration is very efficient because, unlike some other methods, it is safe and permanent; the bound CO_2 is chemically incorporated into the carbonate [4]. Furthermore, mineral deposits are larger than fossil resources, which essentially provides an unlimited supply of the necessary cations (mainly magnesium and calcium) for the process. [5]. There has been much interest in recent years in the use of the mineral olivine for sequestration purposes [6] [7]. This mineral is a good candidate for CO_2 sequestration due to its abundance in the earth's mantle, its lack of aluminium (which tends to produce clays, reducing the number of cations available for carbonation) and because it is a nesosilicate, the silicate group with the lowest ratio of silicon to cations [6].

Olivine is a naturally occurring silicate mineral having the composition $(Mg, Fe)_2 SiO_4$. The name Olivine refers to a range of iron/magnesium silicate minerals, with the composition varying from pure forsterite (Mg_2SiO_4) to pure fayalite (Fe_2SiO_4). Most Olivine falls somewhere between these two extremes, and the Mg and Fe content may occur in any ratio. The process by which olivine sequesters CO_2 is complex; however, it can be simplified as described by the three general reactions as shown in chemical equations (1), (2) and (3):

$$CO_2 + H_2O \leftrightarrow H_2CO_3 \leftrightarrow HCO_3^- + H^+ \leftrightarrow CO_3^{2-} + 2H^+ \quad (1)$$

$$Mg_2SiO_4 + 4H^+ \rightarrow 2Mg^{2+} + H_4SiO_4 \quad (2)$$

$$Mg^{2+} + CO_3^{2-} \leftrightarrow MgCO_3 \quad (3)$$

The first step involves the dissolution of atmospheric carbon dioxide in water, forming carbonic acid, which in turn dissociates and lowers the pH of the system (equation 1). The next reaction (equation 2)

shows the dissolution of the magnesium-rich olivine by acid consumption. The third reaction is the precipitation of magnesium carbonate (equation 3) [7]. Once this process is complete, CO_2 can be stored indefinitely within the magnesite rock. As magnesite is stable it is unlikely to release the bound CO_2 unless subjected to further heating. This process is exothermic and thermodynamically favourable and occurs naturally over geological timescales; however, to be of benefit in the current efforts to reduce the amount of CO_2 in the atmosphere, the process must be accelerated. This may be achieved by raising the reaction temperature, increasing pressure, using a catalyst or decreasing the particle size [8].

Decreasing the particle size of olivine is accomplished through 'mechanical activation' by high energy milling. This process modifies the properties of the olivine beyond merely reducing the particle size and increasing the surface area. It is noteworthy that, during and after activation, the crystal lattice is in a no equilibrium state and the excess energy attributed to disordering contributes to lowering the activation energy of any further reaction of the material [9].

Olivine that is being mined purely for CO_2 sequestration could potentially be made use of in the construction industry as a building material. A number of studies have previously been undertaken to assess the suitability of olivine as a method of solid stabilisation which exploit its ability to sequester CO_2 [10-13].

Here an investigation into the potential for olivine as either an aggregate or, in finely ground form, as a pozzolan in lime-based mortars is presented. An important advantage of olivine additions is increasing the amount of carbonation, and hence CO_2 absorption capacity of the mortar. The widespread use of olivine as an aggregate material has the potential not only to increase the quantity of CO_2 sequestered by lime-based construction materials but also to enhance physical properties. The choice of lime binder for this work is of particular interest because lime mortars have undergone a revival in recent years for conservation work and are now being actively promoted and used in new-build applications [14-15].

There are two potential reaction mechanisms to be investigated: firstly, the dissociation of olivine incorporated into a lime mortar could release Mg^{2+} cations to facilitate the formation of magnesium carbonates. This could potentially result in an increase in the amount of CO_2 absorbed during the hardening phase compared to quartz aggregate and possibly increased strength, as dolomitic limes have been shown to have higher mechanical strength compared to comparable calcitic mortars [16]

[17] secondly, if a pozzolanic reaction occurs, this could help reduce the quantity of lime binder used in a mortar mix.

The choice of binder is an important consideration for the optimal absorption of CO_2. Non-hydraulic lime is the most appropriate material for this type of investigation, as it not only has lower CO_2 emissions during production compared to hydraulic limes due to lower lower temperatures used during production, but it sets purely by carbonation, resulting in a higher quantity of CO_2 being absorbed during the setting phase. Hydraulic lime, by contrast, contains impurities and sets through a combination of carbonation and hydration reactions [18]. The process by which non-hydraulic lime carbonates is described in equations (4) and (5).

Atmospheric carbon dioxide dissolving in water to form carbonic acid

$$CO_2 + H_2O \leftrightarrow H_2CO_3 \quad (4)$$

Calcium hydroxide reacts with carbonic acid to form calcium carbonate

$$Ca(OH)_2 + H_2CO_3 \longrightarrow CaCO_3 + 2H_2O \quad (5)$$

Non-hydraulic lime is available as a lime hydrate or a lime putty. Lime hydrate is a powder, to which sand and water are added to produce the mortar. Lime putty is, as the name suggests, is in the form of a soft putty, which is comprised of approximately 50% water and 50% lime by weight. When a mortar is manufactured using lime putty and sand the water content in the putty is often sufficient to provide a workable consistency and the addition of additional water is not required.

2. Materials

2.1 Lime putty

The binder material used for this work was a calcium hydroxide ($Ca(OH)_2$) lime putty supplied by J J Sharpe which had matured for at least twelve months. Weight measurements of a representative sample of the lime putty were taken before and after water removal by drying in an oven at 100˚C for twenty four hours to determine the solids content. This equated to a solids content of 51%, assumed to be calcium hydroxide. This allowed accurate batching of the mix constituents.

2.2 Olivine

The olivine used was supplied by Industrial Minerals & Refractories Olivine India based in Tamil Nadu, India. The olivine sand received had been derived from Dunite ore and processed using a Raymond three roller mill to grind raw olivine rocks into a sand at an output of approximately 1.25 tonnes per hour. Two different batches of the mineral were received: a fine sand and a coarse sand (Figure 1). The coarse olivine sand was sieved to obtain particles with a maximum size of 2mm to match as closely as possible the standard sand. Chemical composition analysis data from the Material Safety Data Sheets as supplied with the olivine are shown in Table 1. The chemical composition confirms the mineral to be high magnesium, forsteritic olivine.

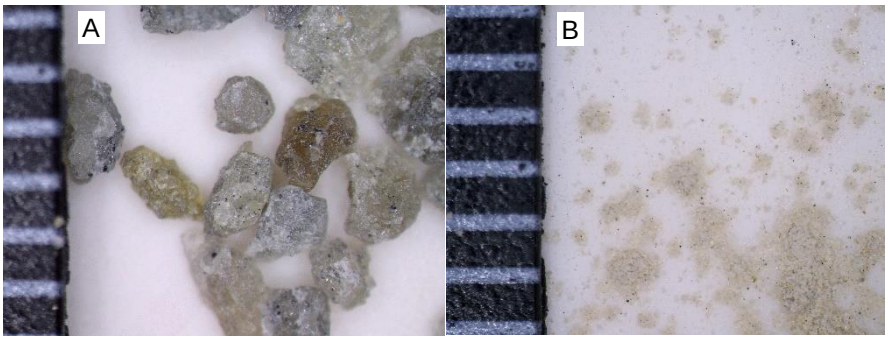

Figure 1: Coarse olivine sand (A) and fine olivine sand (B) shown against a 1mm scale.

Table 1: Chemical composition of olivine

Material	MgO	SiO_2	Fe_2O_3	CaO	Al_2O_3
Coarse olivine sand	49%	21%	8%	1%	-
Fine olivine sand	48.7%	40.2%	8.5%	-	1.2%

The particle size distribution of the fine olivine sand was determined using a Malvern Mastersizer particle size analyser (Figure 2). With the 300mm lens fitted to the Mastersizer, the maximum particle size measurable was 600µm. The data shows that the quantity of particles increases with particle size, up to the limit of 600µm.

The data sheet supplied with the olivine stated that the particles were of size mesh 200# to 300#, which equates to approximately 50 to 74µm. The majority of the particles do fall within this range; however, the peak at approximately 500 indicates some particle agglomeration.

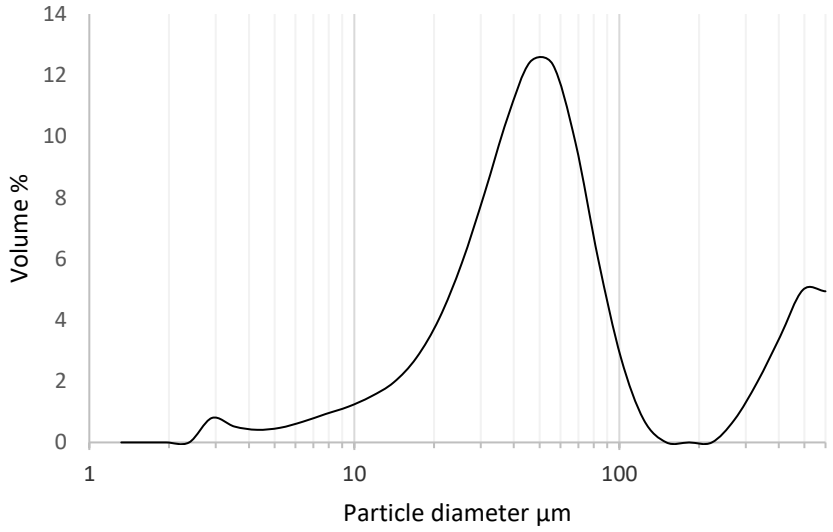

Figure 2: Particle size distribution of the fine olivine sand obtained using the Malvern Mastersizer.

2.3 Standard sand

The sand used in this investigation was a standard dry siliceous natural sand conforming to BS EN 196-1 and ISO 679: 2009. This grade of sand comprises particles that are generally isometric and rounded in shape with the particle size distribution shown in Figure 3. This type of sand was specified for this investigation to facilitate consistency and repeatability of experimental conditions.

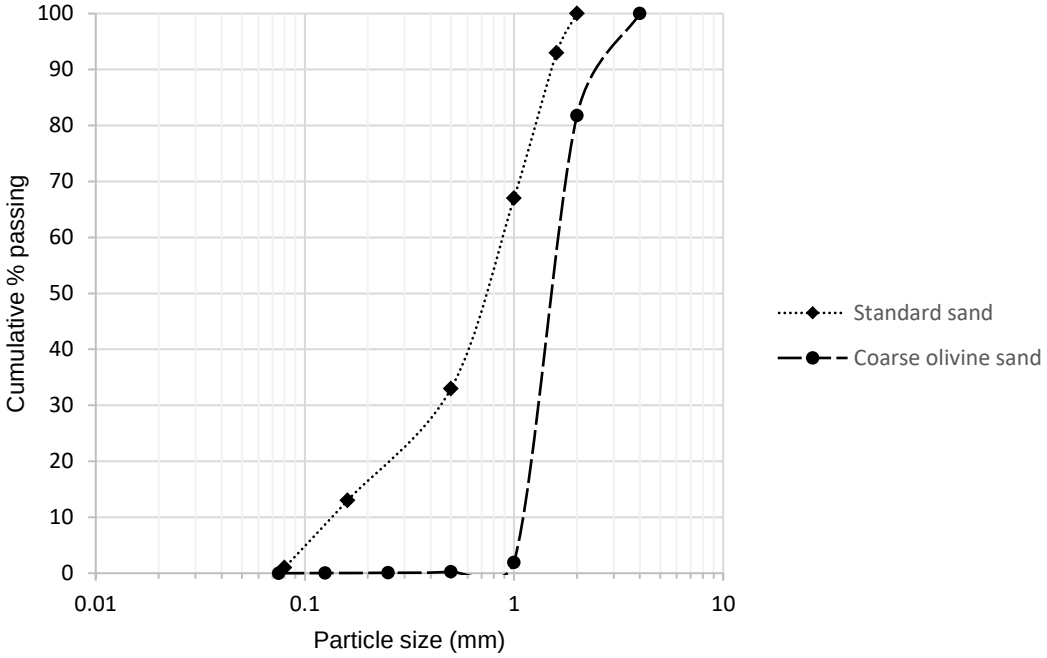

Figure 3: Particle size distribution for stndard sand and large particle olivine obtained by sieve analysis

3. Methods

3.1 Sample preparation

Four different experimental mixes (Table 2) were prepared:

1. S0 – Lime putty binder and standard sand aggregate (2:1)
2. S1 – Lime putty binder and fine olivine sand aggregate (2:1)
3. S2 – Lime putty binder and fine olivine sand aggregate (3:1)
4. S3 – Lime putty binder aggregate and coarse olivine sand (2:1)

The lime and aggregate were prepared using a paddle mixer for a minimum of twenty minutes to ensure the mortar was suitably workable. The experimental mixes were then added to 18 x 38mm cylindrical moulds in small quantities and tamped down as the material was added, to reduce the

occurrence of trapped air bubbles within the specimens. After moulding, the specimens were stored in a climate chamber regulated at a constant temperature of 20ºC ± 2ºC and relative humidity of 65% ± 5% as specified in standard EN 1015-11:1999. The specimens were covered with a thin plastic wrap for the first week to maintain a high level of humidity, as exposure to ambient atmospheric conditions during this period can result in significant reduction in strength due to premature drying and subsequent cracking. The specimens were then left in the moulds for a further week to allow them to achieve sufficient rigidity to facilitate demoulding.

Table 2: Composition of experimental mixes by volume

Specimen	Nominal aggregate: binder ratio	Lime putty (cm^3)	Standard sand (cm^3)	Fine olivine sand (cm^3)	Coarse olivine sand (cm^3)	Bulk density Kg/m^3
S0	2:1	1,000	1,000	-	-	1,504
S1	2:1	1,000	-	1,000	-	1,309
S2	3:1	1,000	-	2,000	-	1,325
S3	2:1	1,000	-	-	1,000	1,515

3.2 Thermodynamic modelling

The thermodynamic modelling software GEM-Selektor v.3 (GEMS3) was used to predict the phase assemblages resulting from lime/olivine mixes. The objective was to predict whether using olivine as an aggregate could theoretically consume more carbon dioxide, through the formation of carbonate phases when compared to a conventional mix of lime and standard sand. Also, the modelling was applied to predict whether the formation of hydration products such as C-S-H was thermodynamically favourable.

For the purposes of this modelling exercise it was necessary to make certain assumptions:

- The (open) thermodynamic system was considerd to comprise of mortar only.
- The small iron content of the olivine, approximately six percent, was not taken into account; the olivine was assumed to be pure fosterite.
- The model assumes that the olivine sand completely dissociates.

Modelling relates to a system where equilibrium conditions are achieved.

The GEMS3 geochemical modelling programme uses an advanced convex programming method of Gibbs energy minimisation implemented as an efficient Interior Points Method. The software can be used to model a single reaction, or as a series of reactions in the form of a phase assemblage diagram [19][20][21].

3.3 X-ray diffraction

Powder X-ray diffraction was carried out using a BrukeraxsD8 Advance X-ray diffractometer equipped with a super speed PSD Vantec-1 detector and Cu K_α X-ray source of wavelength 1.5418Å. Data was collected over the 2θ range from 5° to 60° at a step size of 0.016° and time per step of 424.8s.

3.4 Raman spectroscopy

Raman Spectroscopy was carried out on specimen S2 at 28 days. A Renishaw InVia Raman Spectrometer was used employing a laser of wavelength 532nm. Streamline image acquisition allowed a 1 x 6mm scan of the surface to be obtained. 100% laser power of 80mW was used for 10 second exposures with a slit of 65µm and a 5x objective. The wavelength centre was 1000 giving a data range of 61 to 1835cm^{-1}. The Raman data obtained from the scan were analysed using Renishaw WiRE 4.4 (Windows Raman Environment) software.

3.5 Scanning electron microscopy (SEM)

Scanning electron microscopy was used to examine the physical condition of the specimens. Of particular interest was the occurrence of unreacted olivine particles and bonding between any olivine particles and carbonate phases. Specimens were analysed using a JEOL 6480 LV scanning electron microscope equipped with an Oxford Instruments INCA X-act X-ray detector (silicon drift detector offering a high count rate and reduced operation time).

3.6 Field emission scanning electron microscopy (FESEM)

Field emission scanning electron microscopy was used to examine the morphology of the binder and aggregate at high magnification. Specimens were coated with a 20nm layer of chromium using a Quorum Q150TS machine. A JEOL JSM-6301F microscope was used with an accelerating voltage of 5kV to obtain images with magnification ranging from 10,000x to 20,000x.

3.7 Thermogravimetric analysis (TGA)

TGA analysis was carried out on a sample of each of the two experimental lime/olivine mixes using.a Setaram TG-92 with an open alumina crucible and nitrogen as the purge gas. The test was run over a temperature range of 0 - 1000˚C, in 20˚C steps and 2 minutes per step.

3.8 Mechanical strength testing

Mechanical strength testing was performed using a 50kN Instron 3369 Universal motorised load frame based on BS EN 1015-11:1999 to test compressive strength. Bluehill 3 software monitored and recorded the load on the specimen as a function of extension throughout the test.

4. Results

4.1 Thermodynamic modelling

Figure 4 shows the phase assemblage calculated by the thermodynamic modelling program. The program was used to model the mortar mix S1 as used in the physical tests. The x axis shows the composition of the aggregate, which was maintained at a constant mass of 1,744 grams, but varied from pure quartz sand to pure olivine sand.

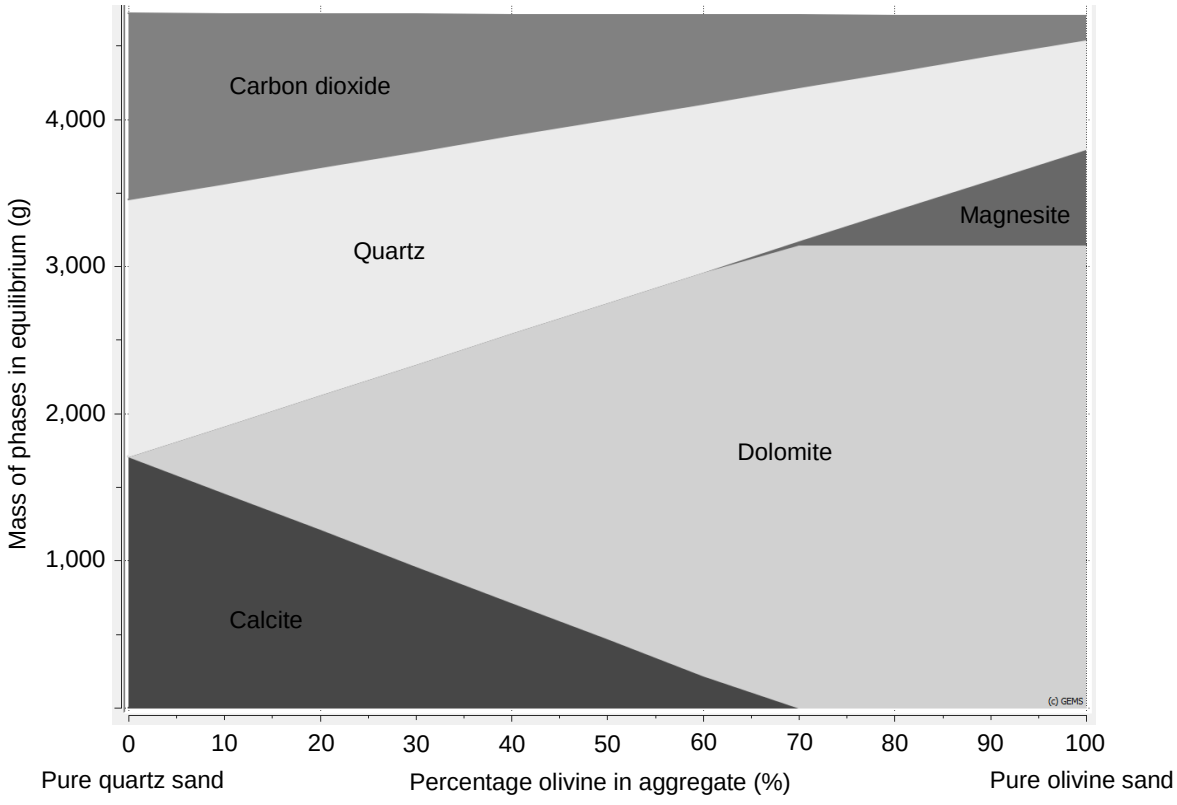

Figure 4: Phase assemblage diagram calculated by the GEMS3 Selektor thermodynamic modelling software for the olivine – lime system.

The results shown are for the reactions at equilibrium when the forsterite will have completely dissociated into magnesium and silica ions; therefore forsterite does not appear in the diagram. The results show that as the proportion of olivine in the aggregate increases, the amount of dolomite increases, indicating that increasing amounts of magnesium ions become available from the dissociated olivine to undergo carbonation.

4.2 X-ray diffraction

XRD was carried out on the raw olivine as received and on the mortar mixes comprising olivine and lime binder in order to confirm the reactions taken place between the olivine aggregate and lime binder.

Figure 5 shows the XRD spectra obtained for the fine olivine sand (A) and the coarse olivine sand (B). They both show high intensity peaks at 2θ values of approximately 23.0, 35.9 and 36.6˚, confirming these to be high magnesium (fosteritic) olivine. The absence of a peak at 31.6 indicates the lack of any significant quantity of iron silicate.

The XRD patterns for the lime/olivine mortar mixes (S2 and S3) show peaks corresponding to the presence of forsterite, calcite and portlandite. The presence of portlandite indicated that the specimen had not completely carbonated, which also accounts for the low intensity peaks for calcite. Dolomite and magnesite could not be positively identified from the data as their high intensity peaks at approximately 32.5˚ and 31˚ respectively, which are close to strong forsterite peaks.

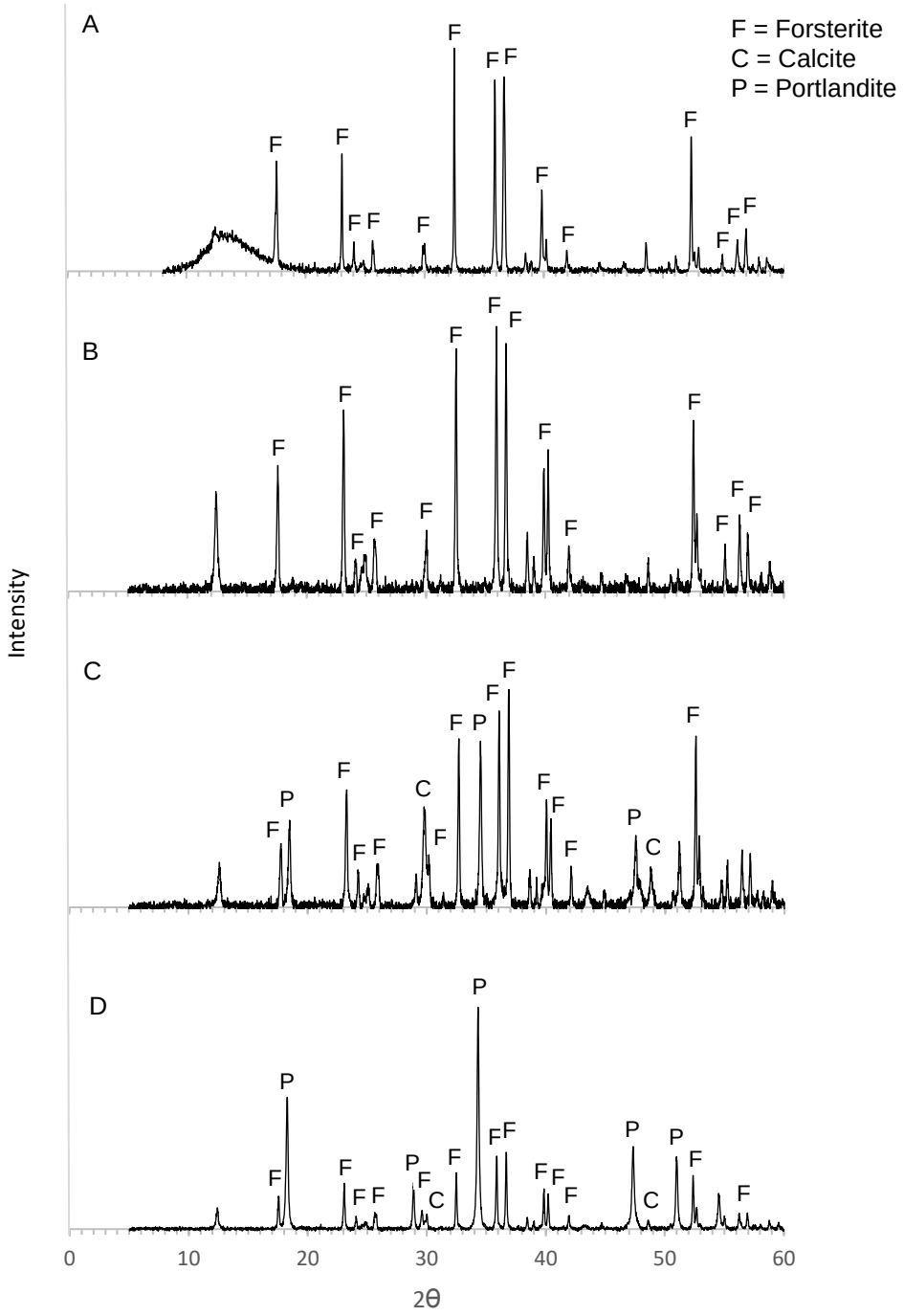

Figure 5: X-ray diffraction (XRD) patterns for fine olivine sand (A), coarse olivine sand (B), mortar mix S2 (C) and mortar mix S3 (D)

4.3 Raman spectroscopy

The S2 specimen was analysed to determine what reactions had taken place between the olivine and the lime and how closely they were in agreement with the results obtained using the thermodynamic software. The 1 x 6mm Raman scan produced 35,478 spectra. These spectra were interrogated using the Renishaw Wire 4.4 program to search for instances of the phases predicted by the thermodynamic

software: calcite ($CaCO_3$), dolomite ($CaMg(CO_3)_2$), magnesite ($MgCO_3$), and quartz (SiO_2). The data were also searched for instances of forsterite (Mg_2SiO_4), which would indicate incomplete dissolution of the olivine. The analysis dentified spectra for calcite, dolomite, magnesite, forsterite and quartz (Figure 6). The data were also interrogated to try and identify the presence of any calcium silicate hydrates (C-S-H). Analysis failed to identify the presence of Tobermorite or Jennite phases, in agreement with the results obtained from the thermodynamic software.

The spectrum in Figure 6(A) shows a spectrum that strongly correlates to calcite, with a strong peak at 1085 cm^{-1}, which is attributed to v_1 symmetric stretching of the CO_3 group and medium intensity peaks at 280, 157 cm^{-1}, which are assigned to v_2 lattice vibrations. Two low intensity peaks at 824 and 854 cm^{-1} indicate a small quantity of olivine in the specimen. Figure 6(B) shows a spectrum from an area of the specimen comprising mainly unreacted olivine. The two high intensity peaks at 822 and 856 cm^{-1} are characteristic of forsteritic olivine and are assigned to the SiO_4 internal stretching vibrational modes. The lower intensity peaks at 1085 and 280 cm^{-1} indicate the presence of some calcite in this area. Figure 6(C) shows the presence of dolomite and calcite together. The peaks at 1085 and 280 identify the calcite. The high intensity peak at 1098 cm^{-1} is a characteristic symmetrical stretching mode for dolomite, and the lower intensity peaks at 300 and 175 cm^{-1} are assigned to the dolomite lattice vibration mode. The spectrum shown in Figure 6(D) is believed to show the presence of magnesite. The high intensity peak at 1095 cm^{-1} is characteristic of the symmetric stretching mode of the carbonate group in magnesite. The lower intensity peak at 325 cm^{-1} is assumed to be the lattice vibration mode peak for magnesite, which is somewhat shifted from its expected position of approximately 330 cm^{-1}. There were not found to be any alternative phases to which this peak could be assigned, given the chemical composition of the specimen under test. The peaks at 202 and 459 cm^{-1} in Figure 6(E) indicate the presence of quartz. This is consistent with the thermodynamic software prediction that quartz should be produced from the dissociation of olivine.

The distribution of each of these minerals within the binder is shown in Figure 7. The lighter areas of the image represent the highest concentration of the mineral being detected.

.

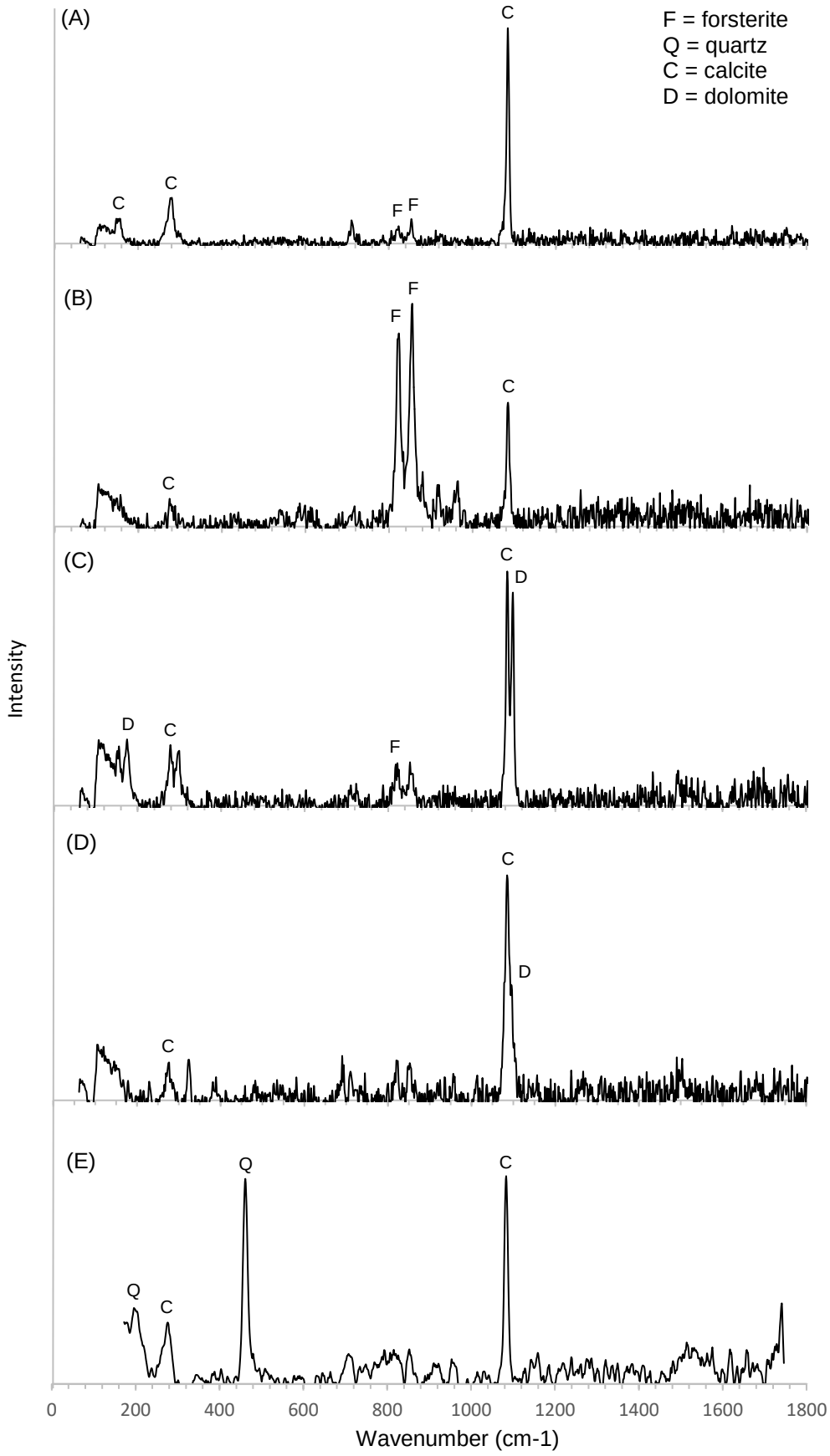

Figure 6: Raman spectra obtained from surface scan of mortar specimen S2 confirming presence of calcite (A), forsterite (B), dolomite (C) magnesite (D) and Quartz (E)

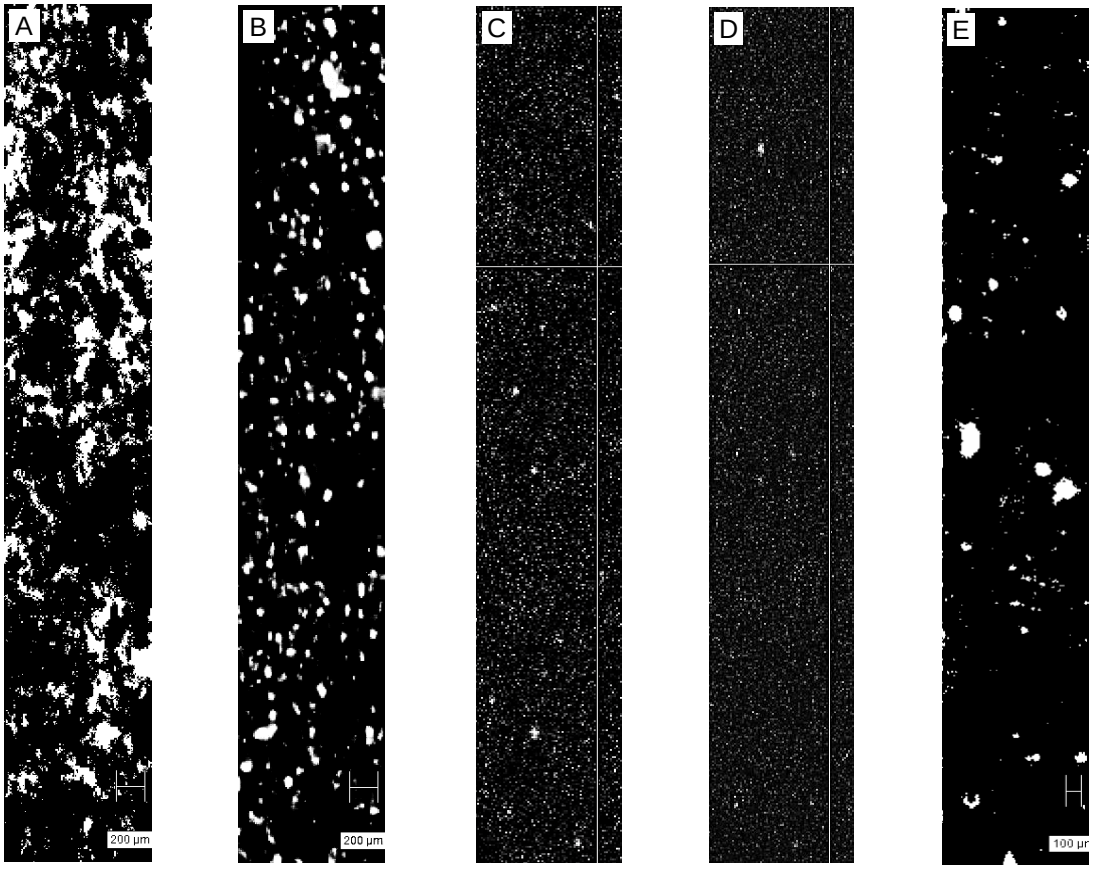

Figure 7: 1 x 6mm Raman scan of S2 specimen surface showing the phase distribution of calcite (A), forsterite (B), dolomite (C), magnesite (D) and quartz (E)

4.4 Scanning electron microscopy and field emission scanning electron mictroscopy

Lower magnification images (up to 5,000X) were obtained using SEM, and FESEM was used to obtain higher resolution images. The images in Figure 8 show the three different types of aggragate used. Images (A) and (B) are of standard sand and show the typical rounded shape of the particles. The fine olivine sand seen in images (C) and (D) shows a much more angular shape and rough surface condition, which is typical of the conchoidal fracture associated with olivine. Images (E) and (F) show the coarse olivine sand particles, which are also rounded in shape but show the typical conchoidal fracture faces.

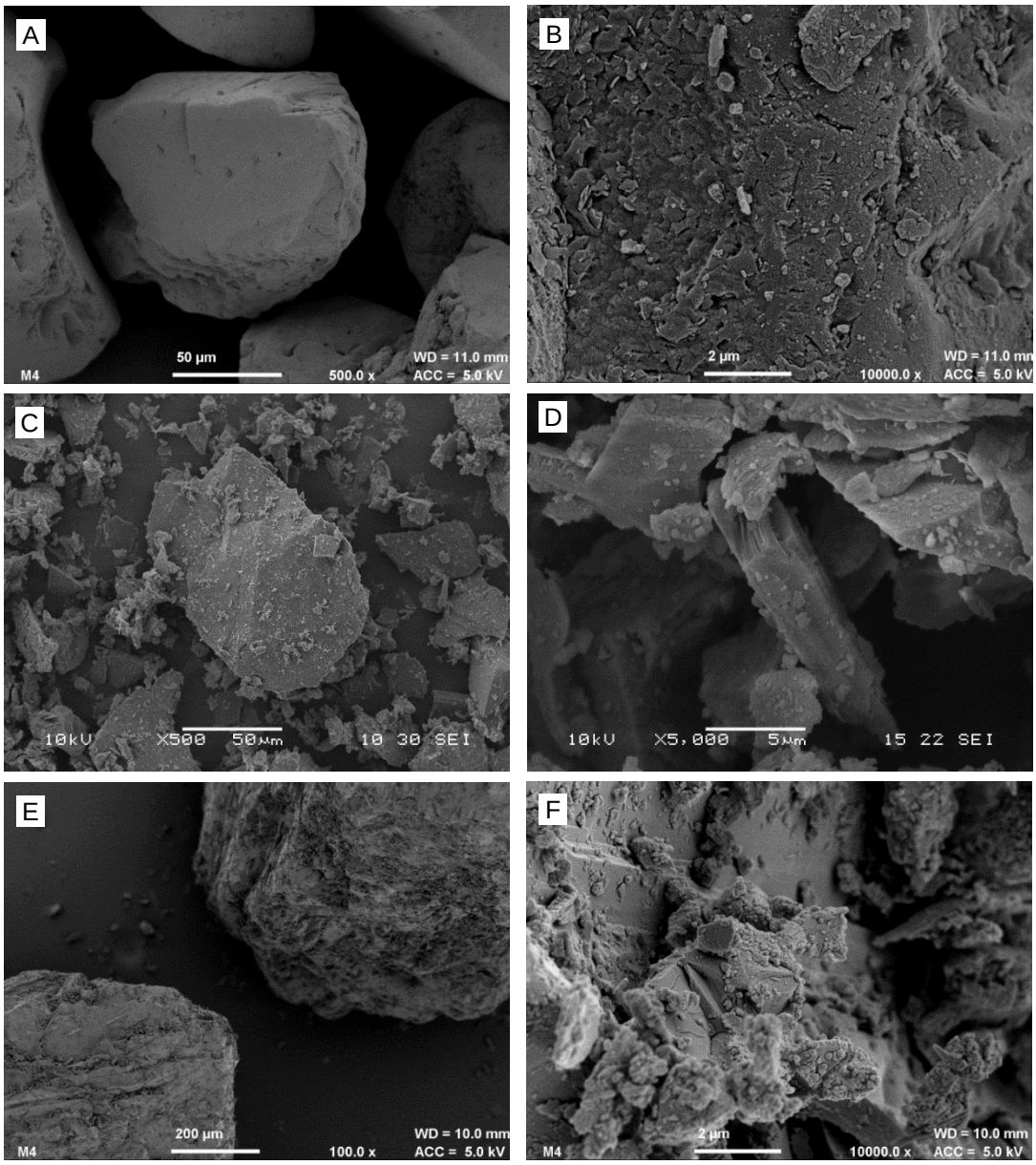

Figure 8: Morphology of aggregate particles – standard sand (A) (B), fine olivine sand (C) (D) and coarse olivine sand (E) (F).

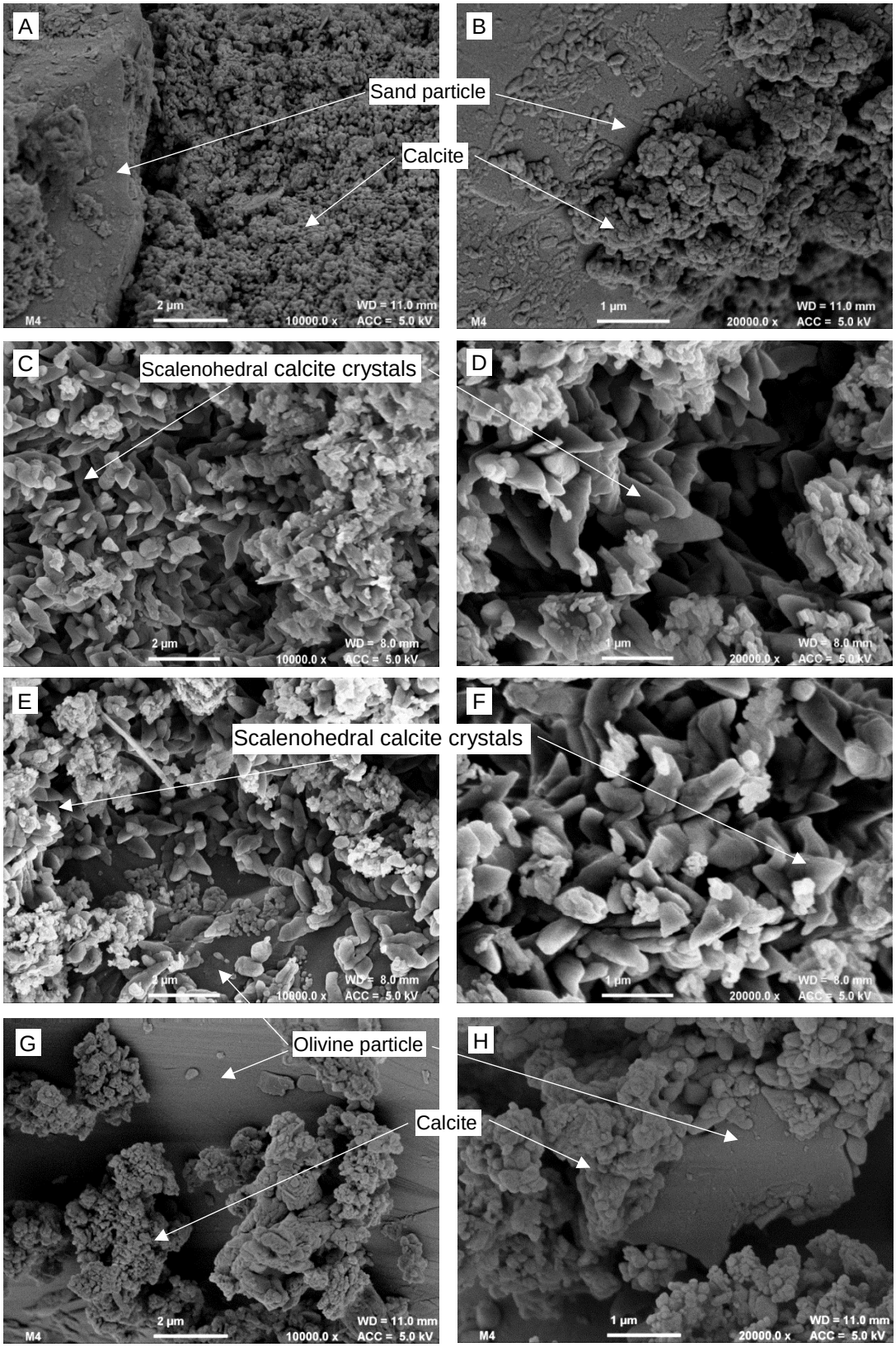

Figure 9: Images of experimental mortar mixes S0 (A)(B), S1 (C)(D), S2 (E)(F) and S3 (G)(H).

The images in Figure 9 show the widespread occurence of well-formed scalenohedral calcite crystals throughout the mortars containg the fine olivine sand aggregate (C)(D)(E)(F). Images of the two mortars containing standard sand and large particle sand aggregates (A)(B)(G)(H) show more granular or massive calcite formations. In the images showing both fine and coarse olivine sand (E)(F)(G)(H), unreacted olivine particles can be seen.

4.6 Thermogravimetric analysis

TGA analysis was carried out on all four mixes. Two distinct instances of mass loss (Figure 10) were observed in each case. The smaller mass loss curve occurred between approximately 420 and 460°C, and this was attributed to dehydration of portlandite. The largest mass loss occurred between approximately 700 and 800°C, which is a result of the decomposition of carbonate material [22] [23].

The equipment was not sufficiently accurate enough to distinguish between the different carbonate phases; however, it can be seen that the mortars containing olivine sand aggregate were shown to contain the highest proportion of carbonate material. In specimen S0 the percentage carbonate of the material that decomposed was 69.1%. In specimens S1, S2 and S3 it was 79.5%, 83.1% and 86% respectively.

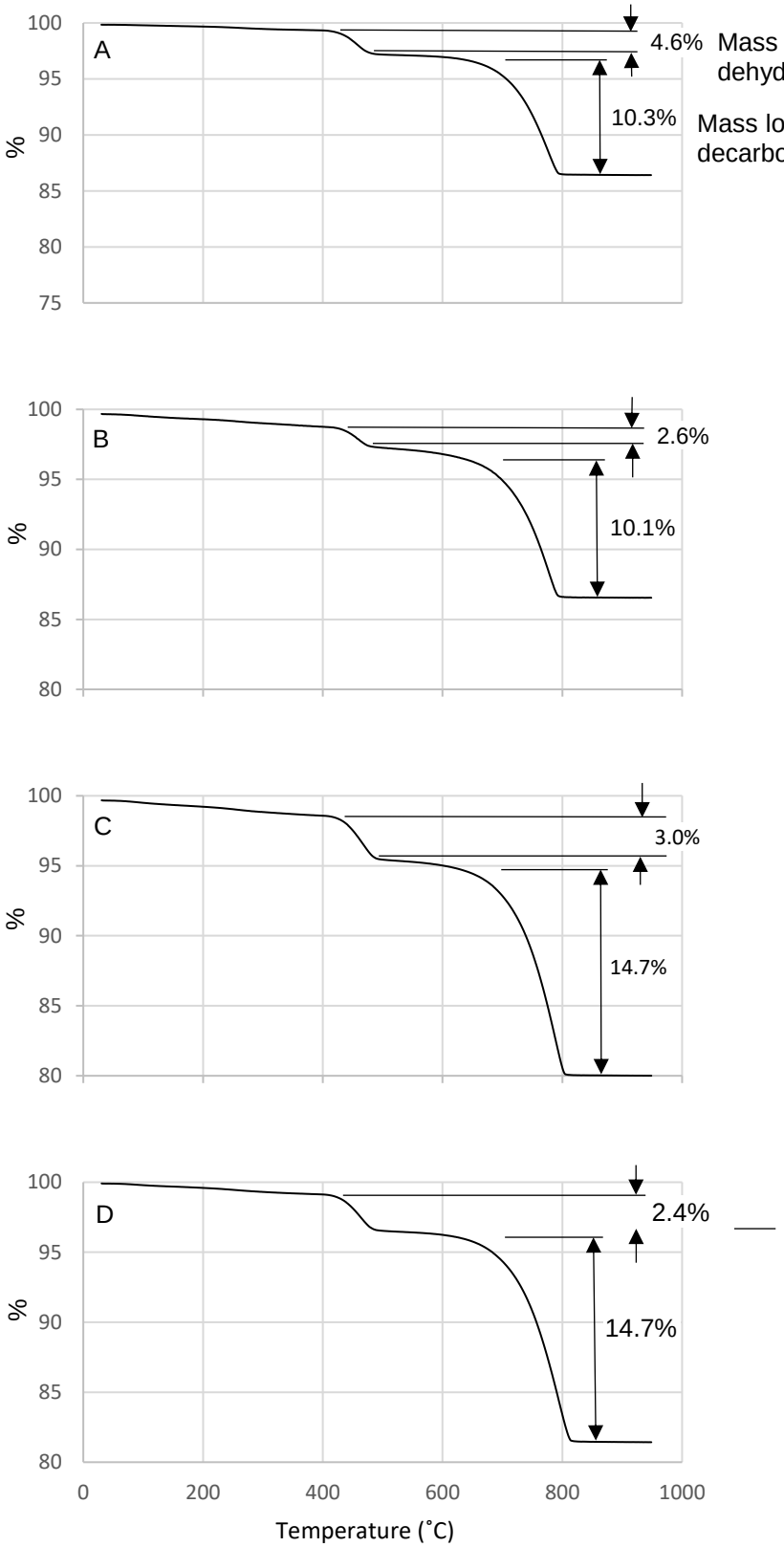

Figure 10: TGA curves for each mortar mix. S0 (A), S1 (B), S2 (C) and S3 (D).

4.7 Mechanical strength testing

Figure 11 shows the compressive strength at twenty eight days for each of the four mortar mixes. The reference mortar comprising lime and sand (S0) achieved a level of strength that would be considered typical for a non-hydraulic mortar at twenty-eight days [24]. However, the specimens incorporating fine olivine sand as aggregate(S1 and S2) obtained compressive strength values that were 278% and 370% higher than with conventional sand. Significantly, the specimen with the highest olivine content (S2) obtained the greatest strength. The specimen comprising lime and coarse olivine sand was the weakest of the mixes.

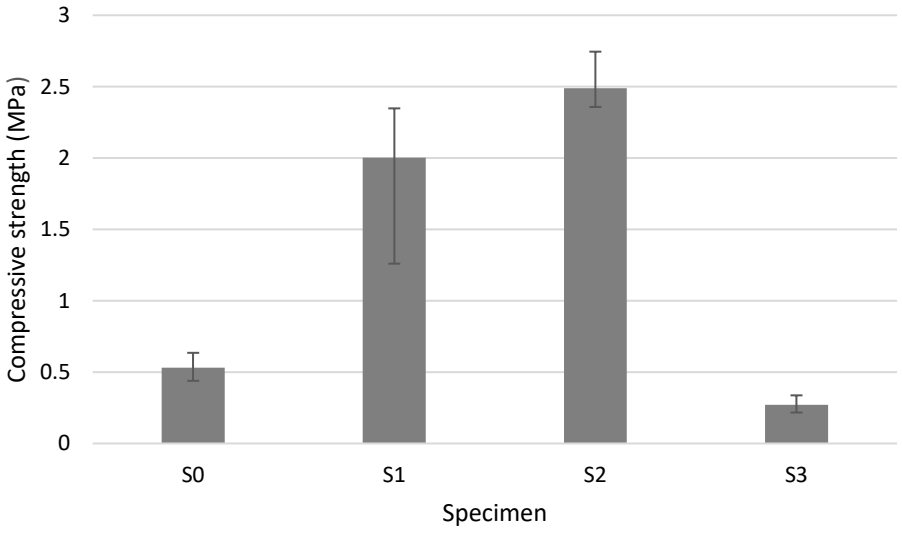

Figure 11: 28 day compressive strength test results for the four experimental mixes; SO=lime and standard sand, S1=lime and fine olivine sand 2:1, S2=lime and fine olivine sand 3:1, S3=lime and coarse olivine sand.

5. Discussion

The research described here has shown conclusively that olivine aggregate, in finely divided form, will react in the presence of lime and water to produce magnesium carbonates, which not only increase the amount of CO_2 absorbed by the mortar during setting, but also provide an enhancement of strength.

The thermodynamic model shows that, at equilibrium, when olivine is the sole aggregate, there should theoretically still be a significant amount of quartz within the system. This can be attributed to new quartz forming from the silica anions released by the dissolution of the olivine. In the experimental mixes, there is significantly less quartz present due to the fact that the system has not reached equilibrium and the olivine has not completely dissociated.

The diagram also shows that as the proportion of olivine aggregate is increased, the total mass of the carbonate phases (calcite, dolomite and magnesite) at equilibrium increases as the olivine dissociates to leave magnesium cations free to form increasing amounts of magnesium carbonates (dolomite and magnesite), and this in turn results in a corresponding increase in CO_2 consumption, as seen by the decreasing amount of CO_2 within the system as the proportion of olivine is increased. Magnesite is only shown to be formed when the aggregate comprises 75% or higher of olivine. The increase in carbonate products when olivine is present can be accounted for by the fact that olivine is a neosilicate and the most reactive mineral on the Goldich dissolution series, whereas quartz is the least reactive and can be considered inert [25]. The model did not predict the production of any hydration products.

The physical tests carried out during this investigation exhibited varying degrees of agreement with the thermodynamic modelling. Although the phases present agree with the thermodynamic software predictions, the quantities present were somewhat different. This is explained by the fact that the software calculated the minerals present at equilibrium, as if the olivine had completely dissociated and reacted with the lime. However, it can be seen from both the XRD and Raman data that there remains a significant quantity of unreacted olivine still present in the mortar. As the quantity of olivine that dissociated was small, the amount of magnesium carbonates (dolomite, magnesite) produced was correspondingly small, which left much of the portlandite free to carbonate and accounts for the large proportion of calcite detected.

The phases identified by Raman spectroscopy aligned more closely with those predicted by the thermodynamic software compared to phases identified from XRD studies. This may be due to the nature of the sample material under test. The XRD samples comprised small amounts of material (20 – 80mg) which was ground into a powder. This sample, therefore, contained material both from the surface and from the bulk, which would account for the presence of unreacted lime (portlandite) from deeper within the specimen. In contrast, Raman spectra were obtained from the surface of the material only where the reactions initiated, which is consistent with the absence of portlandite. The dissociation of the olivine and the carbonation of the lime binder may continue as more water is added to the system over time.

In the absence of any hydration products such as C-S-H, the increased strength of the mixes incorporating olivine can be attributed to the creation of increased amounts of carbonates as shown by

the model and by the XRD and Raman spectroscopy analysis. The specimen with a lime binder to fine olivine aggregate ratio of 1:3 (S2) exhibited a significantly greater strength when compared to the specimen comprising the same materials at a 1:2 ratio (S1). As specimen S2 contained a higher proportion of carbonate material, this provides further support to the inference that higher compressive strength is correlated with higher carbonate content.

The higher carbonate content of the mortars containing fine olivine sand is consistent with the crystal structures identified with the electron microscopy images. The well-formed scalenohedral crystal structures in specimens S1 and S2 indicate that during carbonation there was room for these crystals to grow unconstrained, which provided pathways for CO_2 and water vapour diffusion. Specimens S0 and S3, in contrast, consisted of tightly packed granular carbonate crystals, which would be less condusive to carbonation.

Results support the hypothesis that strength increases obtained with olivine aggregate can be attributed to increased carbonation however structural differences suggest that there may also be physical effects. For example, the shape and surface morphology of small particle olivine is substantially different from that of the large particle olivine and the normal silica sand. The small olivine particles are very angular in shape and have rough surfaces, both of which are conducive to higher strength due to bonding between the aggregate and the lime paste. The lower strength of the mix containing coarse olivine sand must be attributed to the larger particles of olivine possessing lower strength compared to the fine olivine sand, which could be due to the more intense milling required to obtain the smaller particles.

6. Conclusions

This research has, for the first time, investigated the effect of using olivine as an aggregate in lime mortars. The following conclusions may be drawn:

- Olivine sand will dissociate in a lime mortar mix to facilitate the formation of magnesium carbonates, increasing CO_2 absorption.
- The total carbonate content of aged mortars containing fine olivine sand aggregate is greater than that found in a conventional silica sand lime mortar of similar mix proportions that contains a purely silica sand aggregate.

- The increased formation of carbonates when olivine aggregates are used promotes a greater compressive strength of 2.5 MPa compared to conventional mortar mixes 0.5 MPa incorporating quartz sand aggregate.
- The particle size of the olivine sand and corresponding surface area, is of significance in promoting the necessary dissociation and carbonation reactions.

References

[1] IPCC, 2014. Climate Change 2014 Synthesis Report. Geneva, 2014

[2] Papayianni, I., Papachristoforou, M., Patsiou, V., Petrohilou, V, 2013. *Development of fire resistant shotcrete with olivine aggregates*. IABSE Symposium, May 6 2013 Rotterdam 2013: Assessment, Upgrading and Refurbishment of Infrastructures, pp. 246-252.

[3] Pesce, G. L., Fletcher, I. W., Grant, R., Molinari, M., Parker, S. C. and Ball, R. J., 2017. Carbonation of Hydrous Materials at the Molecular Level: A Time of Flight-Secondary Ion Mass Spectrometry, Raman and Density Functional Theory Study. *Crystal Growth and Design*, 17 (3), pp. 1036-1044.

[4] Lackner, K. S., Wendt, C. H., Butt, D. P., Joyce, E. L., Sharp, D. H., 1995. Carbon Dioxide disposal in Carbonate Materials. *Energy,* 20(11), pp.1173-1170.

[5] Lackner, S. J., 2003. A Guide to CO2 Sequestration, *Science*, 300, p.1677

[6] Fasihnikoutlab, M. H., Westgate, P., Huat, B. B. k., Asadi, A., Ball, R. J., Nahazanan, H. and Singh, P, 2015. New Insights into Potential Capacity of Olivine in Ground Improvement. *Electronic Journal of Geotechnical Engineering,* 20[2015], pp.2137-2148

[7] Fasihnikoutlab, M. H., Asadi, A., Huat, B. B. K., Westgate, P., Ball, R. J., and Pourakbar, S., 2016. Laboratory-scale model of carbon dioxide deposition for soil stabilisation. *Journalof Rock Mechanics and Geotechnical Engineering,* 8[2016], pp.178-186

[8] Olsson, J., Bovet, N., Makovicky, E., Bechgaard, K., Balogh, Z., Stipp, S. L. S., 2011. Olivine reactivity with CO2 and H2O on a microscale: Implications for carbon sequestration. *Geochimica et Cosmochimica Acta*, 77(2012), pp.86-97.

[9] Tove, A.H. 2010. *Dissolution and carbonation of mechanically activated olivine.* Thesis (PhD). Norwegian University of Science and Technology, Trondheim.

[10] Demirbas, A., 2006. Carbon Dioxide Disposable via Carbonation. *Energy Sources, Part A: Recovery, Utilisation and Environmental Effects,* 29(1) pp59-65

[11] Tkacova, K., 1989. *Mechanical activation of minerals.* Amsterdam: Elsever Science Publishers

[12] Fasihnikoutalab, M. H., Asadi, A., Unuler, C., Huat, B. K., Ball, R. J. and Pourakbar, S., 2017. Utilization of Alkali-Activated Olivine in Soil Stabilization and the Effect of Carbonation on Unconfined Compressive Strength and Microstructure. *ASCE Journal of Materials in Civil Engineering*, 29 (6), 06017002.

[13] Fasihnikoutalab, M., Pourakbar, S., Ball, R. and Huat, B., 2017. The Effect of Olivine Content and Curing Time on the Strength of Treated Soil in Presence of Potassium Hydroxide. *International Journal of Geosynthetics and Ground Engineering*, 3 (12).

[14] Fasihnikoutalab, M., Asadi, A., Huat, B., Westgate, P., Ball, R. and Pourakbar, S., 2016. Laboratory-scale model of carbon dioxide deposition for soil stabilisation. *Journal of Rock Mechanics and Geotechnical Engineering*, 8 (2), pp. 1078-186.

[15] Fasihnikoutalab, M., Westgate, P., Huat, B. B. K., Asadi, A., Ball, R., Nahazanan, H. and Singh, P., 2015. New Insights into Potential Capacity of Olivine in Ground Improvement. *Electronic Journal of Geotechnical Engineering*, 20 (8), pp. 2137-2148.

[16] Elert, K., Rodriguez-Navarro, C., Pardo, E. S., Hansen, E., and Cazalla, O., 2002. Lime Mortars for the Conservation of Historic Buildings. *Studies in Conservation,* Vol. 47, No. 1, pp. 62-75

[17] Yates, T., Ferguson, A., 2008. The use of lime-based mortars in new build. Amersham: NHBC Foundation

[18] Arizzi, A., Cultrone, G., 2012. The difference in behaviour between calcitic and dolomitic lime mortars set under dry conditions: The relationship between textural and physical-mechanical properties. *Cement and Concrete Research,* 42 (2012) pp. 818-826

[19] An experimental and computational study to resolve the composition of dolomitic lime Grant, J., Pesce, G. L., Ball, R. J., Molinari, M. & Parker, S. C. 2016 In : RSC Advances. 6, 19, p. 16066-16072 7 p.

[20] Brocklebank, I., ed., 2012. *Building Limes in Conservation.* Shaftsbury: Donhead Publishing Ltd. p.10

[21] GEMS, 2018. *Gibbs Energy Minimization Software for Geochemical Modelling* [online]. Villingen: Paul Scherer Institut. Available from: http://gems.web.psi.ch [Accessed 7 February 2018].

[22] Kulik D.A., Wagner T., Dmytrieva S.V., Kosakowski G., Hingerl F.F., Chudnenko K.V., Berner U. (2013): GEM-Selektor geochemical modelling package: revised algorithm and GEMS3K numerical kernel for coupled simulation codes. *Computational Geosciences* 17, 1-24. doi.

[23] Wagner T., Kulik D.A., Hingerl F.F., Dmytrieva S.V. (2012): GEM-Selektor geochemical modelling package: TSolMod library and data interface for multicomponent phase models. *Canadian Mineralogist* **50**, 1173-1195. doi.

[24] Valverde, J. M., Perejon, A., Medina, S. and Perez-Maquedad, L. A., 2015. Thermal decomposition of dolomite under CO2: insights from TGA and in situ XRD analysis. *Phys. Chem. Chem. Phys*., 2015, 17, p.30166

[25] Wulandari, S. W., Adinata, P. M., and Fajrin, A., 2017. Thermal decomposition of dolomite under CO2-air atmosphere. *AIP Conference Proceedings 1805, 040006 (2017).* American Institute of Physics

[26] Lawrence, R. M. H., 2006. *A Study of Carbonation in Non-Hydraulic Lime Mortars.* Thesis (PhD). University of Bath

[27] Goldich S. S., 1938. A Study in Rock Weathering. *The Journal of Geology*, Vol. 46, No. 1, p.56